Target Detection Algorithm for SAR Image Based on Visual Saliency

Huijie Xie, **Tao Tang**, **Deliang Xiang**, **and Yi Su**
College of Electronic Science and Engineering, National University of Defense Technology, China

Abstract— Based on visual saliency theory and local probability density function statistical feature, a target detection algorithm for SAR image is proposed. Local probability density function statistical feature reflects the difference between target and clutter on human vision. According to local probability density function statistical feature, saliency map of SAR image could be calculated by using hypothesis testing theory and Bayes theorem. Then target detection result could be acquired from saliency map by binary segmentation. For different kinds of real SAR images, target detections are implemented by the proposed algorithm and CFAR algorithm. The comparison of the detection results shows that the proposed algorithm detects all size-fixed targets with lower false alarm rate than CFAR algorithm.

1. INTRODUCTION

Synthetic aperture radar (SAR) is an effective instrument to obtain remote sensing information, which is also widely used on civil remote sensing and military reconnaissance. Maneuvering targets, mainly including vehicle, ship and airplane, are interesting targets on civil remote sensing and military reconnaissance. At the present stage, target detection is one of the hotspots and difficulties on SAR image interpretation, which plays an important role in civil and military application.

Constant false alarm rate (CFAR) algorithm [1–3] is a classical target detection algorithm for SAR image. CFAR algorithm is designed based on the fact that the radar cross section (RCS) of the target is larger than the RCS of the clutter. And CFAR algorithm performs efficiently in single clutter background. However, there are rather false alarms if the background is complex with buildings, trees and shadows.

For the moment, the discriminant ability of human vision system (HVS) is far better than target detection algorithm. HVS performs efficiently in image interpretation and extracts interesting target from background rapidly and effectively. For the past few years, salient region detection technique based on visual attention mechanism has been one of the significant techniques on filtrating and analyzing image data. Imitating HVS, several salient region detection algorithms [4–7] have been proposed. Saliency map [4] has been regarded as common measurement for saliency level. The algorithms based on spatial domain calculate saliency map via image features such as intensity, color, orientation, texture, gray level histogram, etc.. The algorithms based on spectrum domain calculate saliency map via the correlation between salient feature and spectrum domain of the image. However, these algorithms are designed for optical image and they should be improved for SAR image.

Considering SAR image, several ship detection algorithms [8, 9] have been proposed based on visual attention mechanism. However, these algorithms are only suitable for ship detection in sea background and they could not be applied to target detection in complex background without any modification.

In this paper, a target detection algorithm based on visual saliency has been proposed for target detection problem in complex background for SAR image. Local probability density function statistical feature is used for the proposed algorithm, which is sensitive to not only the intensity feature but also the shape and size of the target. According to local probability density function statistical feature, saliency map could be calculated by using hypothesis testing theory and Bayes theorem. And then target detection result could be acquired from saliency map by binary segmentation.

2. DESCRIPTION OF THE PROPOSED ALGORITHM

The main process of the proposed algorithm is as following. First of all, the parameter of the proposed algorithm should be determined according to the sizes of the target. And then, local saliency and global saliency of each pixel should be calculated respectively. Furthermore, saliency map could be acquired by combining local saliency map and global saliency map. At last, target detection result could be acquired from saliency map by binary segmentation.

2.1. Local Saliency Measure

In order to estimate the statistical clutter model accurately, most of CFAR algorithms set guard region between target pixel and clutter region in order to avoid the estimation being affected by target pixels. As a reference, sliding square window W of the proposed algorithm has been divided into, from inside to outside, target region, guard region and clutter region, which is shown in Fig. 1. The side length of target region w_T should be less than or equal to the width of the target in order to make sure that most of pixels in target region are target pixel.

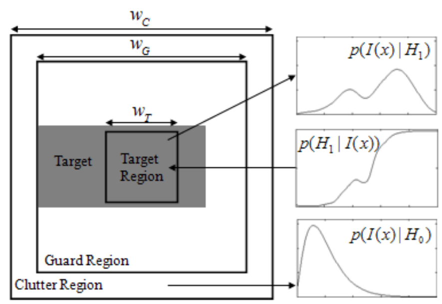

Figure 1: Sketch map of the local saliency measure.

Let $x \in \mathbf{R}^2$ be a pixel in target region and clutter region. And let $I(x)$ to be the intensity value of pixel x. Define two hypotheses as Equation (1).

$$\begin{aligned} &H_0\text{: Pixel } x \text{ is not salient.} \\ &H_1\text{: Pixel } x \text{ is salient.} \end{aligned} \tag{1}$$

And make an initial assumption as Equation (2).

$$\begin{aligned} &H_0\text{: Pixel } x \text{ is not salient.} \quad x \in \text{Clutter Region} \\ &H_1\text{: Pixel } x \text{ is salient.} \quad x \in \text{Target Region} \end{aligned} \tag{2}$$

According to the assumption, conditional probability density function of pixels in target region and clutter region could be estimated.

Based on Bayes theorem $P(A|B) = P(B|A)P(A)/P(B)$, define Equation (3).

$$p(H_1|I(x)) = \frac{p(I(x)|H_1)P(H_1)}{P(I(x))} \tag{3}$$

Since $p(I(x)) = p(I(x)|H_0)P(H_0) + p(I(x)|H_1)P(H_1)$, rewrite Equation (3) to be Equation (4).

$$p(H_1|I(x)) = \frac{p(I(x)|H_1)P(H_1)}{p(I(x)|H_0)P(H_0) + p(I(x)|H_1)P(H_1)} \tag{4}$$

where $P(H_1)$ is the prior probability of assumption H_1 and $P(H_0)$ is the prior probability of assumption H_0. It is obvious that $P(H_0) = 1 - P(H_1)$. Further discussion about H_1 would be shown in Section 3.1. Equation (4) computes the probability of H_1 for each pixel x in target region based on the assumption. Posterior probability $p(H_1|I(x))$ reflects the contrast of the pixels between target region and clutter region. Then define the local saliency measure as Equation (5).

$$S_{local}(x) = p(H_1|I(x)) \tag{5}$$

With the purpose of target detection, rewrite Equation (5) as Equation (6) because of the prior knowledge that target's RCS is larger than clutter's and that target pixel's intensity value is larger than clutter pixel's.

$$S_{local}(x) = \begin{cases} p(H_1|I(x)), & I(x|H_1) \geq \mathrm{E}[I(x|H_0)] \\ \text{Low Value}, & I(x|H_1) < \mathrm{E}[I(x|H_0)] \end{cases} \tag{6}$$

where $\mathrm{E}[I(x|H_0)]$ is the mean value of $I(x)$ in clutter region.

$$\mathrm{E}[I(x|H_0)] = \frac{1}{N}\sum\nolimits_N I(x|H_0) \tag{7}$$

Local saliency measure $S_{local}(x)$ reflects visual saliency of the pixel x in target region in a sliding window. For the target with the length $l_{t\arg et}$ and the width $w_{t\arg et}$, the side length of target region w_T would be set as $w_T = w_{t\arg et}$ and the side length of guard region w_G would be set as $w_G = 2 \times l_{target} - w_{target}$ in order to assure that there is few target pixels in clutter region.

2.2. Global Saliency Measure

Local saliency measure could be calculated in a sliding window. Then global saliency measure should be calculated in the whole image. Redefine clutter region as the whole image except for target region.

$$\begin{aligned} &H_0\text{: Pixel } x \text{ is not salient.} \quad x \notin \text{Target Region} \\ &H_1\text{: Pixel } x \text{ is salient.} \quad x \in \text{Target Region} \end{aligned} \tag{8}$$

Similar to Section 2.1, global saliency measure could be estimated as Equation (9).

$$S_{global}(x) = \begin{cases} p(H_1|I(x)), & I(x|H_1) \geq \mathrm{E}[I(x|H_0)] \\ \text{Low Value}, & I(x|H_1) < \mathrm{E}[I(x|H_0)] \end{cases} \tag{9}$$

where the definitions of $p(H_1|I(x))$ and $\mathrm{E}[I(x|H_0)$are same to Equation (4) and Equation (7). The difference between Equation (6) and Equation (9) is the range of clutter region.

Global saliency measure $S_{global}(x)$ reflects visual saliency of the pixel x in target region in the whole image. For the target with the length l_{target} and the width w_{target}, the side length of target region w_T would be set as $w_T = w_{target}$.

2.3. Saliency Map and Target Detection

Similar to CFAR algorithm, window $W(i)$ would be slid over the whole image with step s_W. Step s_W could be chosen from 1 to w_T. In the proposed algorithm, Step s_W is chosen as $s_W = 0.3 \times w_T$ in order to reduce the amount of calculation and preserve the edge of the target at the same time. Because sliding window $W(i)$ would overlap with each other, saliency measure $S_i(x)$ would be calculated multiple times. As shown in Equation (10), maximum of $S_i(x)$ would be chosen as the saliency measure of pixel x.

$$S(x) = \max_i \{S_i(x)|x \in W(i)\} \tag{10}$$

Using local saliency measure and global saliency measure respectively, local saliency map S_{local} and global saliency map S_{global} could be gained. In both S_{local} and S_{global}, targets possesses higher visual saliency than natural clutter. Therefore, the smaller value of $S_{local}(x)$ and $S_{global}(x)$ would be chosen as the final saliency measure $SaliencyMap(x)$.

$$SaliencyMap(x) = \min(S_{local}(x), S_{global}(x)) \tag{11}$$

In the saliency map, strong scatterer with the same size to target is salient, on the contrary clutter and scatterer with greatly different size of target are not salient. Therefore, target detection result could be easily acquired from saliency map by binary segmentation as shown in Equation (12).

$$Result(x) = \begin{cases} 1, & SaliencyMap(x) \geq T \\ 0, & SaliencyMap(x) < T \end{cases} \tag{12}$$

where T is the threshold value that would be discussed about in detail in Section 3.1.

3. EXPERIMENTAL RESULTS AND ANALYSIS

Experimental SAR images are acquired from the moving and stationary target acquisition and recognition (MSTAR) plan and acquired by project term via airborne X-band SAR.

3.1. Parameters Discussion about Prior Probability and Threshold Value

As shown in Equation (4), a positive correlation is obvious between posterior probability $p(H_1|I(x))$ and prior probability $p(H_1)$. Therefore, firstly prior probability $p(H_1)$ should be determined, and then threshold value T would be determined according to $p(H_1)$.

As shown in Fig. 2(a), it is an airborne X-band SAR image with the size of 684×496. There are 6 vehicle targets and a group of corner reflectors locating at twice kinds of low vegetation. The size of targets is about 39×19. And the group of corner reflectors looks like a circle whose diameter is about 9 pixels.

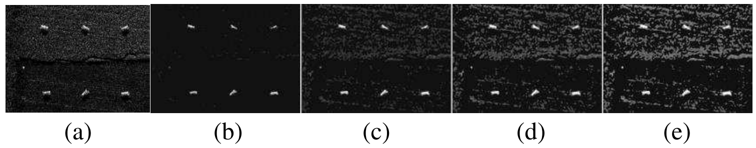

Figure 2: Original SAR image and saliency maps when the prior probability is set as 0.1, 0.2, 0.3, 0.4 respectively. (a) Original SAR image (b) $p(H_1) = 0.1$. (c) $p(H_1) = 0.2$. (d) $p(H_1) = 0.3$. (e) $p(H_1) = 0.4$.

In the experiment, the side length of target region w_T is chosen as 19 pixels. And the prior probability $p(H_1)$ is set as 0.1, 0.2, 0.3, 0.4 respectively. As a result, the saliency maps are shown in Figs. 2(b), (c), (d), (e). It is obvious that targets are more salient when the $p(H_1)$ is smaller. However, when $p(H_1)$ is too small, as shown in Fig. 2(b), the saliency of the target in top right corner has been inhibited because of its slightly incomplete outline. Moreover, the fracture and distortion of the target should be considered in a target detection algorithm for SAR image. According to the discussion as above, the prior probability $p(H_1)$ is chosen as $p(H_1) = 0.2$ in the following experiment.

When $p(H_1)$ is chosen as 0.2, the saliency map is shown in Fig. 2(c). Now the threshold value T is set as 0.6, 0.7, 0.8, 0.9 respectively. As a result, the target detection results are shown in Fig. 3. When $T = 0.6$, all targets have been detected and the group of corner reflectors has been detected as a false alarm. When $T = 0.7$ and $T = 0.8$, there is not false alarm or missing detection. When $T = 0.9$, there are missing detections. Further experiments show that there is not false alarm or missing detection when $T \in [0.64, 0.86]$. This fully shows that targets are far more salient than clutter in the saliency map, and it is easy to detect targets from saliency map by binary segmentation. According to the discussion as above, the threshold value T is chosen as $T = 0.75$ in the following experiment.

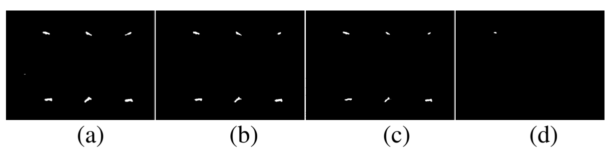

Figure 3: Target detection results when the threshold value is set as 0.6, 0.7, 0.8, 0.9 respectively. (a) $T = 0.6$. (b) $T = 0.7$. (c) $T = 0.8$. (d) $T = 0.9$.

3.2. Experiment with MSTAR Image

As shown in Fig. 4(a), it is a MSTAR image acquired via spotlight X-band SAR with the size of 1472×1784 and the resolution of $0.3\,\mathrm{m} \times 0.3\,\mathrm{m}$. There are 9 vehicle targets marked by circles and 2 unidentified scatterers marked by rectangle locating in the image. The size of targets is about 35×17. The intensity of the unidentified scatterers is almost the same to targets and the sizes of them are quite different to targets. And there are also different kinds of vegetations and shadows in the image.

Experimental parameters are determined according to Section 3.1. Saliency map and target detection result are shown in Fig. 4(b) and Fig. 4(c) respectively. As a result, the proposed algorithm detects all targets without any false alarm or missing detection.

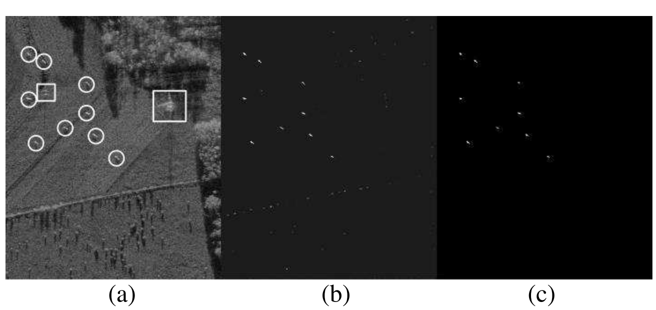

Figure 4: (a) Original MSTAR image. (b) Saliency map. (c) Target detection result.

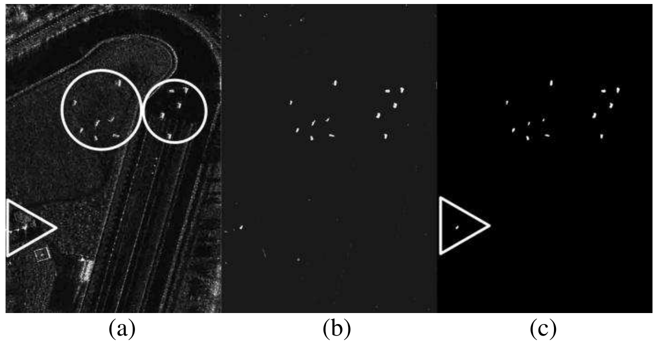

Figure 5: (a) Original airborne SAR image. (b) Saliency map. (c) Target detection result.

3.3. Experiment with Airborne SAR Image

As shown in Fig. 5(a), it is a SAR image acquired via airborne X-band SAR with the size of 587×841 and the resolution of $0.5\,\mathrm{m} \times 0.5\,\mathrm{m}$. There are 12 vehicle targets marked by circles in the image. The size of targets is about 25×11. There are also buildings, corner reflectors, trees, shadows, roadway in the image.

Experimental parameters are determined according to Section 3.1. Saliency map and target detection result are shown in Fig. 5(b) and Fig. 5(c) respectively. The proposed algorithm detects all targets without any missing detection but a false alarm. The false alarm marked by triangle is a strong scatterer with the similar size to the target. However, there is not false alarm caused by clutter.

3.4. Comparison Experiment and Analysis

The CFAR algorithm is implemented for these SAR images and the constant false alarm rate is set as 0.1%. The comparison between the proposed algorithm and CFAR algorithm is shown in Table 1. The comparison shows that the proposed algorithm detects all targets with lower false alarm rate than CFAR algorithm. Since single pixel is judged in CFAR algorithm, mini size strong scatterer, such as corner reflector, must be detected as false alarm. In the proposed algorithm, conditional probability density function $p(I(x)|H_1)$ corresponding to mini size scatterer is comparatively small, so the saliency of mini size scatterer would be inhibited.

The step of sliding window of the proposed algorithm is $s_W = 0.3 \times w_T$, and that of CFAR algorithm is $s_{CFAR} = 1$. The ratio of the proposed algorithm to CAFR algorithm on calculation times is $\eta = (2 \times s_{CFAR}^2)/s_W^2 \approx 22/w_T^2$. As for these SAR images, the proposed algorithm is far more efficient than CFAR algorithm.

Table 1: The comparison between two target detection algorithms.

	Image type	Detection rate	False alarm rate	Computing time/(s)
The proposed algorithm	Simple image	100%	0%	11.4
	MSTAR image	100%	0%	169.7
	Airborne SAR image	100%	8.3%	246.8
CFAR algorithm	Simple image	100%	16.7%	146.1
	MSTAR image	100%	211.1%	1833.1
	Airborne SAR image	100%	125%	921.3

4. CONCLUSION

In this paper, a target detection algorithm for SAR image based on visual saliency has been proposed by connecting visual saliency theory with target detection theory. This algorithm is appropriate for target detection in a SAR image with complex background, and solves the problem of CFAR algorithm that mini size strong scatterer must be detected as false alarm. As for target detection in a high resolution SAR image, the proposed algorithm has advantages such as high detection rate, low false alarm rate and fast computing.

REFERENCES

1. Di Bisceglie, M. and C. Galdi, "CFAR detection of extended objects in high-resolution SAR images," *IEEE Trans. on Geoscience and Remote Sensing,* Vol. 43, No. 4, 833–843, Apr. 2005.
2. Morgan, C. J., L. R. Moyer, and R. S. Wilson, "Optimal radar threshold determination in Weibull clutter and Gaussian noise," *IEEE Aerospace and Electronic Systems Magazines*, Vol. 11, No. 3, 41–43, Mar. 1996.
3. Gao, G., "A parzen-window-kernel-based CFAR algorithm for ship detection in SAR images," *IEEE Geoscience and Remote Sensing Letters*, Vol. 8, No. 3, 557–561, May 2011.
4. Itti, L., C. Koch, and E. Niebur, "A model of saliency-based visual attention for rapid scene analysis," *IEEE Trans. on Pattern Analysis and Machine Intelligence*, Vol. 20, No. 20, 1254–1259, Nov. 1998.
5. Harel, J., C. Koch, and P. Perona, "Graph-based visual saliency," *Advances in Neural Information Processing Systems*, Vol. 19, 545–552, 2007.
6. Hou, X. D. and L. Q. Zhang, "Saliency detection: A spectral residual approach," *IEEE Conference on Computer Vision and Pattern Recognition*, 1–8, Minneapolis, 2007.
7. Rahtu, E. and J. Heikkila, "A simple and effficient saliency detector for background subtraction," *IEEE 12th International Conference on Computer Vision Workshops*, 1137–1144, Kyoto, 2009.
8. Yu, Y., B. Wang, and L. M. Zhang, "Hebbian-based neural networks for bottom-up visual attention and its applications to ship detection in SAR images," *Neurocomputing,* Vol. 74, 2008–2017, 2011.
9. Hou, B., W. Yang, W. Shuang, et al., "SAR image ship detection based on visual attention model," *IEEE International Geoscience and Romote Sensing Symposium*, 2003–2006, Melbourne, 2013.